https://doi.org/10.5194/egusphere-2024-3468
Preprint. Discussion started: 11 December 2024

Source-explicit estimation of brown carbon in the polluted atmosphere over North China Plain: implications for distribution, absorption and direct radiative effect

Jiamao Zhou[1,2], Jiarui Wu[1], Xiaoli Su[1], Ruonan Wang[1], Xia Li[1], Qian Jiang[1], Ting Zhang[1], Wenting Dai[1], Junji Cao[3], Xuexi Tie[1], Guohui Li[1]

[1]Key Laboratory of Aerosol Chemistry and Physics, State Key Laboratory of Loess and Quaternary Geology, Institute of Earth Environment, Chinese Academy of Sciences, Xi'an 710061, China

[2]Guanzhong Plain Ecological Environment Change and Comprehensive Treatment National Observation and Research Station, Xi'an 710061, China

[3]Institute of Atmospheric Physics, Chinese Academy of Sciences, Beijing 100029, China

Correspondence to: Guohui Li (ligh@ieecas.cn)

https://doi.org/10.5194/egusphere-2024-3468
Preprint. Discussion started: 11 December 2024

Abstract. Brown carbon (BrC) is recognized as a considerable factor changing the atmospheric radiation balance. In addition to the combustion of biomass and biofuel sources, both field observations and laboratory studies suggest that fossil fuels is an important contributor to BrC. This highlights a critical gap in the treatment of BrC in climate models, which typically categorize organic aerosols (OA) from fossil fuels as non-absorbing or simplistically assume that all OA are light-scattering. Here we present a regional simulation of BrC during a highly polluted winter in North China Plain (NCP) by using the WRF-Chem model incorporating currently known BrC sources with explicit absorption properties. The modified model generally performs well in simulating air pollutants and aerosols species against observations. Our simulations show that the average near-surface mass concentration of BrC in the NCP is 4.8 μg m^{-3} and its contribution to the aerosol absorption optical depth at 365 nm is 11.2%. A diagnostic adjoint method has been used to quantify the overall direct radiative effect (DRE) of BrC and contributions from various sources. We find that the DRE of BrC is predominantly negative with an average of -0.10 W m^{-2} at the top of the atmosphere (TOA) over the NCP, and consequently decreases the direct radiative cooling effect of OA by 24.0 % with a TOA warming of up to +0.34 W m^{-2}. Our findings reveal that residential coal combustion is the principal contributor to the DRE of BrC in the NCP, and a noteworthy contribution from secondary BrC.

Key words: Brown Carbon, emission sources, absorption, direct radiative effect

https://doi.org/10.5194/egusphere-2024-3468
Preprint. Discussion started: 11 December 2024

1 Introduction

Brown Carbon (BrC) is a collective component for those colored organic compounds with wavelength dependent light-absorption properties (Mukai and Ambe, 1986; Kirchstetter et al., 2004; Andreae and Gelencsér, 2006). BrC has been recognized as an important short-lived climate forcer contributing considerably to climate change by warming of the atmosphere (IPCC, 2013; Feng et al., 2013; Jacobson, 2014; Jo et al., 2016; Brown et al., 2018). The light absorption induced by BrC can be equal to or even higher than that of black carbon (Pokhrel et al., 2017), and substantially influences atmospheric radiative forcing. Recent studies have shown that BrC counts 30%~50% of the total absorption of aerosols in Atlanta USA, Brazil and Hebei China (Hoffer et al., 2006; Yang et al., 2009; Liu et al., 2013). The direct radiation effect (DRE) caused by BrC is greater than +1 W m^{-2} in some regions, such as South Asia, Africa and Southeast Asia, much higher than the global average (Park et al., 2010; Feng et al., 2013; Lin et al., 2014; Saleh et al., 2014; Jo et al., 2016; Wang et al., 2018; Yan et al., 2018). As a result, BrC reduces the cooling effect caused by organic aerosols by approximately 16% (Jo et al., 2016). However, the model evaluated DRE associated with BrC is highly uncertain with order of magnitude difference, e.g., the estimated global DRE of BrC is in the range between +0.03 W/m^2 to +0.57 W/m^2 (Hammer et al., 2016), which is caused by the limited of BrC mass and absorption properties observations (Tuccella et al., 2020; Saleh, 2020).

Currently, the sources and chemical composition of BrC is not completely understood yet. Most of observations in the world indicate that biomass burning (BB), bio fuels (BFs) combustion, and ageing of secondary organic aerosol (SOA) are the much of BrC sources (Hecobian et al., 2010; Shapiro et al., 2009; Bond et al., 2013). Only a few climate models have assumed that primary OA from BB and BFs combustion is the main or sole BrC (Feng et al., 2013; Jacobson, 2014; Saleh et al., 2014; Hammer et al., 2016; Brown et al., 2018), and aromatic SOA is added in some recent studies (Jo et al., 2016; Wang et al., 2018; Zhang et al., 2020). Generally, fossil fuels (FFs) combustion is taken for nonsignificant BrC source. OA from FFs combustion is assumed to be non-absorbing and not accounted for in current climate models. However, a growing number of laboratory and field studies have demonstrated that low-efficiency FFs combustion is proved to be an indispensable source of BrC (Bond, 2001; Saleh, 2020), especially for the areas where coal is the main energy. According to the National Bureau of Statistics of China (https://data.stats.gov.cn), coal consumption in 2014 is about 4000 Tg, accounting for 65.8% of the total primary energy of China, ~93 Tg of which is used as fuel of households. The poor burning conditions and limited emission control facilities have caused massive emissions of organic particles (Yan et al.,

https://doi.org/10.5194/egusphere-2024-3468
Preprint. Discussion started: 11 December 2024

2017; Yan et al., 2022). Recent field observations have shown that residential coal combustion (RCC) is an important source of BrC in northern China (Wang et al., 2019; Tian et al., 2019; Wang et al., 2021) and the fossil source contributes much more in northern China than in other parts of the world (Mo et al., 2021), which is not involved in previous climate models. Xie et al. (2019) have concluded that BrC from RCC is the main contributor of the aerosol light absorption during the wintertime in Beijing, with the contribution of 48%-55%. In addition, several studies have indicated that vehicle emissions are also a nonnegligible BrC source (Du et al., 2014; Hu et al., 2017; Xie et al., 2017a; Tang et al., 2020; Wang et al., 2021; Huang et al., 2022).

These recent findings indicate a critical gap on the treatment of BrC in climate models. This includes expanding the scope of BrC sources and assigning distinct optical properties for each source and incorporating those that have been underrepresented or overlooked in past assessments into numerical models. In this study, we include the main primary emission sources (RCC, BB, BFs, vehicle emissions) of BrC and secondary BrC in a regional model, the Weather Research and Forecasting model coupled with Chemistry (WRF-Chem). A representative region, North China Plain (NCP), is chosen as the study domain with high anthropogenic carbonaceous aerosols due to the widespread use of coal and biomass burning for heating during winter and the increasing number of motor vehicles. We have performed a month simulation to evaluate the surface distribution, absorption and the DRE of BrC in the NCP, by updating BrC optical properties of different sources. Sensitivity experiments have also been devised to assess the contribution of BrC from major sources.

2 Model and Method

2.1 WRF-Chem Model and configurations

The WRF-Chem model (Grell et al., 2005; Fast et al., 2006) modified by Li et al., (2010; 2011a; 2011b; 2012) is used to quantitatively estimate the BrC in the NCP. A heavily polluted month from January 1 to 30, 2014 is selected for the simulation period. The anthropogenic emissions are developed by Zhang et al. (2009) and Li et al. (2017), including five sources contributed from agriculture, industry, power generation, residential, and transportation sources. The biogenic emissions are calculated online using the MEGAN (Model of Emissions of Gases and Aerosol from Nature) model developed by Guenther et al. (2006). Additionally, the grid-based RCC, BB and BFs combustion emissions are used to update the BrC sources in this study which will be described later. The model simulation domain is shown in Fig. 1. The detailed model description and configurations can be found in supplementary text S1.1 and Table S1, respectively.

https://doi.org/10.5194/egusphere-2024-3468
Preprint. Discussion started: 11 December 2024

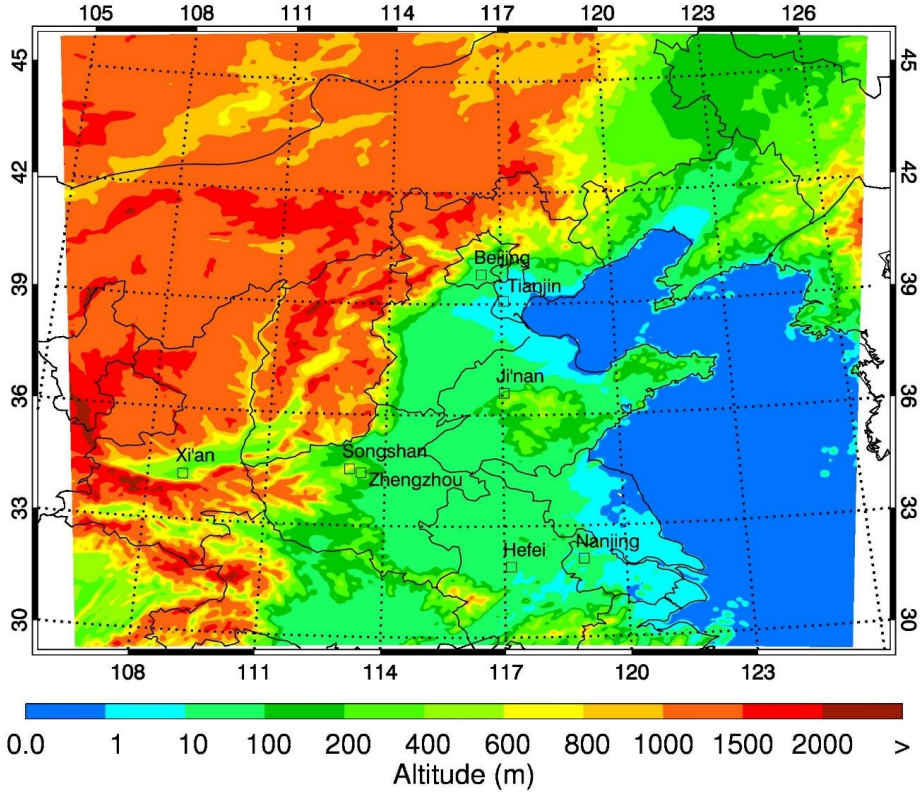

Figure 1. WRF-Chem simulation domain with topography. The square denotes the field sites for simulation and observation comparison

2.2 Aerosol radiative module

Goddard shortwave module (Chou and Suarez, 1999) is used to study the DRE of BrC, which takes into account the extinction by water vapor, ozone, oxygen, carbon dioxide, aerosols, Rayleigh scattering, and clouds. The aerosol radiative module has been incorporated into the WRF-Chem model to calculate the aerosol optical depth (AOD), single scattering albedo (SSA), and the asymmetry factor which are used to the Goddard module. Four types of aerosol are classified as (1) internally mixed sulfate, nitrate, ammonium, hydrophilic organics and black carbon (BC), and water; (2) hydrophobic organics; (3) hydrophobic BC; and (4) other unidentified aerosols (generally dust-like aerosols), which are assumed to be mixed externally. The detailed calculation method can be found in Li et al. (2011a) and the supplementary text S1.2. The BrC in the model has an effective density of 1.2 g cm^{-3} for primary BrC and of 1.0 g cm^{-3} for secondary BrC. The imaginary refractive index of BrC is discussed in 2.3.2.

https://doi.org/10.5194/egusphere-2024-3468
Preprint. Discussion started: 11 December 2024

2.3 Model modifications

2.3.1 Source separation of BrC

The definition of BrC in the model is dependent on its sources. Due to lack of BrC emission inventories, most of the previous studies either simply use OA from BB as a proxy of BrC or estimate the emission of BrC based on the emission ratio of BrC versus BC (Zhu et al., 2021). According to the characteristics of energy structure in China, assumptions and code modifications of the WRF-Chem model have been made to consider the primary BrC from different sources. These involve three separated primary BrC sources, including BB emissions, fossil fuel emissions from RCC and on-road vehicles (FFs-TRA), and a part of SOA which has light absorption property whereas other types of POA and SOA is assumed to be purely scattering. In this study, BB source corresponds to open fire, household biomass burning and biofuel consumption emissions.

Up to now, the study for BrC emissions is limited (Sun et al., 2017; Sun et al., 2021; Wang et al., 2022). Quantifying emission factors of BrC is still challenging due to the need to isolate BrC from other pollutants, and the factors vary greatly depending on the methods and proxies used. There are usually two methods to estimate the emissions of BrC, one is the traditional inventory method, and the other is calculating by using the ratio of BrC to other combustion products like BC. The gap between these two methods, even the same method, could be very wide. Sun et al., (2017; 2021) reported that the BrC from RCC and BB emission is 592 Gg and 712 Gg, respectively in 2013 in China but it likely to be biased low because of the proxy of BrC. Whereas Zhu et al., (2021)obtained a large RCC emissions (2.42 Tg $year^{-1}$) by using the emission ratio method. In the present work, we have taken consideration of the observation results that fossil sources significantly contribute to water soluble organic carbon (WSOC), especially in colder seasons, and that both the contribution and light absorption efficiency of WSOC are higher in northern China than in southern China (Feng et al., 2013; Mo et al., 2021). Follow on this study, we use a proportion of OA from different sources to estimate the emission of BrC. RCC is responsible for about 45% of primary BrC emissions which resulting an annual emission of 616 Gg in the NCP. While all the BB emissions of OA are considered to be absorption, contributing approximately 45% to primary BrC emissions which is 664 Gg per year in NCP. The vehicle emissions of BrC is based on the calculations made by Wang et al., (2022), about 84 Gg $year^{-1}$ in this study. The total yearly BrC primary emissions in the NCP is over 1364 Gg $year^{-1}$ which is closer to the estimation of traditional inventory method. Figure 2 shows the contributing regions and burdens of the three separated primary sources of BrC. SOA has also shown light absorption in the atmosphere (Lin et al., 2014). According to previous studies, the BrC from SOA is generally

https://doi.org/10.5194/egusphere-2024-3468
Preprint. Discussion started: 11 December 2024

produced from oxidation of biogenic and aromatic volatile organic compound (VOC) precursors (Liu et al., 2015; Liu et al., 2016; Xie et al., 2017b). Some models designate the fraction of aromatic SOA to the total as the secondary BrC, such as the study by Wang et al. (2014), which set this proportion at 8%. In this work, a proportion of 10% of the total SOA is included as a part of BrC. Applying the emission fractions above, OA is split into white scattering POA, white scattering SOA and BrC at each time step.

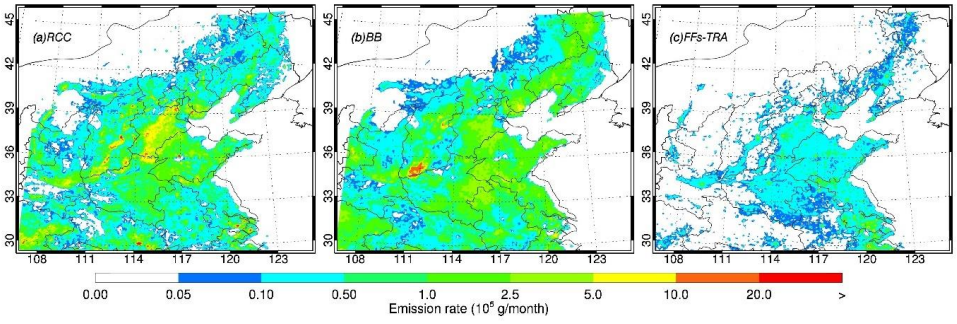

Figure 2 Monthly BrC emissions burdens in January 2014 in NCP from FFs-coal, BB and FFs-traffic.

2.3.2 BrC optical properties

The refractive indices of BrC as a function of wavelength are used for radiative transfer calculations. The complex refractive index ($m = n + ik$) of aerosol components enables practical implementation in the model, where n is the real part primarily associated with the scattering efficiency, and k is the imaginary part primarily associated with the absorption efficiency (Bohren and Huffman, 1998). The real part of BrC refractive index is the same of non-absorbing OA which is fairly constrained with reported values typically ranging from 1.5 to 1.7 (Saleh et al., 2014; Browne et al., 2019; Li et al., 2020). In this study, it follow the study by Li et al. (2011a) and Wu et al. (2020). The imaginary part (k) of BrC refractive index exhibit strong wavelength dependence and the values range over several orders of magnitude (Saleh et al., 2018; Sengupta et al., 2018). Limited studies on the optical properties of BrC from fossil fuel combustions are reported at present. The average MAE of RCC at 365nm is ranging from 0.80 m^2 g^{-1} to 2.47 m^2 g^{-1} (Yan et al., 2017; Li et al., 2019; Tang et al., 2020; Wang et al., 2020; Ni et al., 2021; Song et al., 2021; Wang et al., 2021). Considering that BrC has a high light absorption efficiency in northern China during cold season (Mo et al., 2021), we choose a field measurement of MAE in the wavelength range between 370 nm and 660 nm, showing that the changes in anthropogenic emissions affect the optical properties of BrC (Zhang et al., 2022). This MAE is higher than that reported by Ni et al., (2021) and Xie et al., (2017a) to implement the absorption of BrC. The MAE of SOA follows the suggestion made by Ni et al., (2021) .

https://doi.org/10.5194/egusphere-2024-3468
Preprint. Discussion started: 11 December 2024

The value of k in this work is derived from the measured MAE using the following Eq.(1) (Liu et al., 2013; Lu et al., 2015) as shown in Table 1:

$$k_{BrC,\lambda} = \frac{\rho \times \lambda \times MAE_{\lambda}}{4\pi} \quad (1)$$

Where MAE_{λ} ($m^2\ g^{-1}$) is the bulk mass absorption efficiency of BrC at the corresponding wavelength λ. ρ (g cm^{-3}) is the density of organic aerosols, which is assigned as 1.2 g cm^{-3} in this study.

Table 1 The refractive index of BrC used in the model

Aerosols	Wavelength (nm)	k	References
BrC-RCC	370	0.1890	Zhang Y. 2022
	470	0.0608	
	520	0.0272	
	590	0.0173	
	660	0.0081	
BrC-BB	370	0.0587	
	470	0.0219	
	520	0.0120	
	590	0.0092	
	660	0.0046	
BrC-FFs-Tra	370	0.0509	
	470	0.0194	
	520	0.0085	
	590	0.0046	
	660	0.0018	
BrC-SOA	365	0.00490	Ni et al., 2021
	500	0.00070	

2.3.3 Shortwave direct radiative effect calculation and experimental design

The shortwave DRE calculations of BrC follow the method reported by Chen et al (2021) as shown in Eq. (2). The DRE of BrC is calculated by the difference between the net radiant flux with and without BrC, where the net radiant flux is the difference between the downward $(F_{\downarrow})$ and upward radiant flux $(F_{\uparrow})$.

$$DRE_{TOA} = (F^{a}_{\downarrow TOA} - F^{a}_{\uparrow TOA}) - (F^{0}_{\downarrow TOA} - F^{0}_{\uparrow TOA}) \quad (2)$$

Where DRE_{TOA} represent the shortwave DRE at the top of the atmosphere (TOA). F^{a} and F^{0} is the radiant flux with and without BrC aerosols, respectively.

A adjoint methodology proposed by Zhao et al (2013) and Huang et al (2015) has been used to diagnose the optical depth and DRE of BrC aerosols. Optical properties and radiative transfer of different sources BrC are

https://doi.org/10.5194/egusphere-2024-3468
Preprint. Discussion started: 11 December 2024

calculated multiple times with one or a group of aerosol mass removed or without BrC absorption from each of calculation as the following Eq. (3) and Eq. (4). In addition, the model also takes into account the reduced aerosol masses along with the change in aerosol number concentration and size distribution.

$$AOD_{[species\ i]} = AOD_{[all\ species]} - AOD_{[without\ species\ i/without\ species\ i\ absorption]} \quad (3)$$

$$DRE\ Forcing_{[species\ i]} = DRE\ Forcing_{[all\ species]} - DRE\ Forcing_{[without\ species\ i/without\ speices\ i\ absorption]} \quad (4)$$

This method is more efficient than the traditional approach of running the model multiple times with the exclusion of a specific aerosol component. It not only saves computational time but also provides a more accurate estimation focused solely on the direct radiative effect of aerosols.

3 Results and Discussions

3.1 Model performance

Before evaluating the DRE of BrC further, results from the standard simulation are used to validate the model performance. Using available measurements, we first validate the spatial distribution and temporal variation of air pollutants ($PM_{2.5}$, O_3, NO_2, SO_2) in the NCP, the temporal variation of downward shortwave flux at the surface (SWDOWN) in Beijing, Tianjin, Zhengzhou, Hefei and Ji'nan, and the temporal variation of aerosol species (OA, elemental carbon, ammonium, sulphate and nitrite) in Beijing, Tianjin and primary OA from BB, RCC, motor vehicles and SOA in Beijing in January, 2014. The detailed data descriptions and quantitative statements of model biases can be found in supplementary text S2.1 and S3. In general, the model reasonably well simulates the air pollutants, SWDOWN, and aerosol species against measurements.

The daily AOD at 550 nm (AOD_{550}) from the dataset of Long-term Gap-free High-resolution Air Pollutant (LGHAP), derived via tensor-flow-based multimodal data fusion (Bai et al., 2022), is compared with the simulation. Figure 3a and 3b shows the pattern comparison of the monthly simulated and retrieved AOD_{550}. The model reasonably reproduces the AOD distribution compared to the retrieval in the NCP, but slightly underestimates the AOD_{550}. The monthly simulated and retrieved AOD_{550} is 0.45 and 0.48 on average in the NCP, respectively. Figure 3c shows the scatter plot of the daily simulated and retrieved AOD_{550} averaged in the NCP during the simulation period. The simulated daily average AOD_{550} correlates quite well with the retrieval, with a regression slope of 1.05 and correlation coefficient of 0.82. Generally, the retrieved and simulated AOD increases with deterioration of the particulate pollution. Figure 4 provides the pattern comparison of the simulated and Ozone Monitoring Instrument (OMI) retrieved AOD at 440 nm (AOD_{440}) averaged during the simulated episode.

https://doi.org/10.5194/egusphere-2024-3468
Preprint. Discussion started: 11 December 2024

The simulated AOD_{440} pattern is generally in agreement with the retrieval, but the underestimation still exists. The average simulated and retrieved AOD_{440} is 0.50 and 0.53 in the NCP, respectively. In brief, the model generally performs well in simulating the AOD distribution, but is subject to underestimating AOD. It worth noting that the simulated AOD is not only dependent on the column aerosol content and composition, also substantially influenced by relative humidity (RH) which determines the aerosol hydroscopic growth. Additionally, the satellite retrieved AOD is subject to contamination by existence of clouds, and considering the high occurrence frequency of clouds during haze days, the retrieved AOD is generally higher than the simulation (Satheesh et al., 2010; Chand et al., 2012).

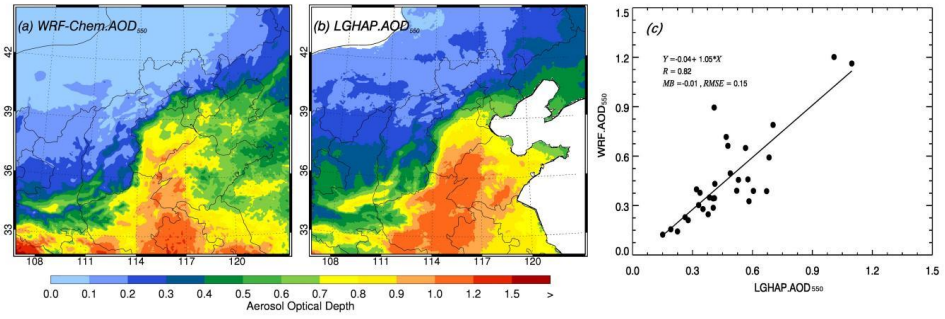

Figure 3 (a) monthly simulated AOD_{550} of WRF-Chem, (b) monthly retrieved AOD_{550} of reanalysis dataset LGHAP, and (c) scatter plot of the daily simulated and retrieved AOD_{550} averaged in the NCP from 01 January to 30 January 2014

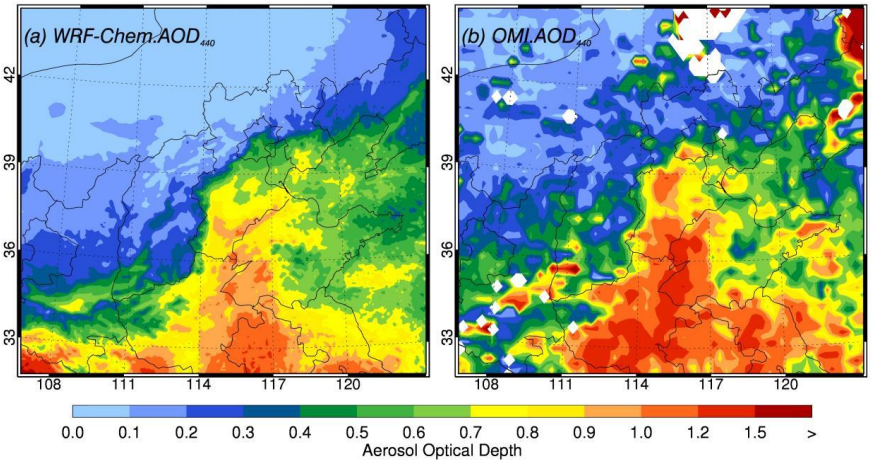

Figure 4 (a) monthly simulated AOD_{440} of WRF-Chem, (b) monthly retrieved AOD_{440} of OMI in the NCP from 01 January to 30 January 2014

https://doi.org/10.5194/egusphere-2024-3468
Preprint. Discussion started: 11 December 2024

SSA determines the strength of aerosols in absorbing solar radiation. Figure 5 shows the comparisons of simulated versus observed SSA at 440 nm (SSA_{440}) at Sun-sky radiometer Observation NETwork (SONET) sites including Beijing, Songshan, Xi'an, Hefei, Nanjing in January 2014. Due to the influence of clouds, the observational data from SONET are not continuous, consequently, a total of 237 valid data points are available for comparison. The model tends to underestimate SSA_{440} with a MB of -0.04. The relationship indicates that the model might predict more absorbing aerosols or underestimate RH. Meanwhile, the uncertainties of the simulated SSA can be caused by other factors, such as mixing state of aerosols, particle shape, wavelength, and mass ration of non-black carbon to BC (Liu et al., 2017). Jeong et al. (2020) have proposed that the density of BC is an important factor for the SSA estimation, and dust size distribution reduces SSA_{440}.

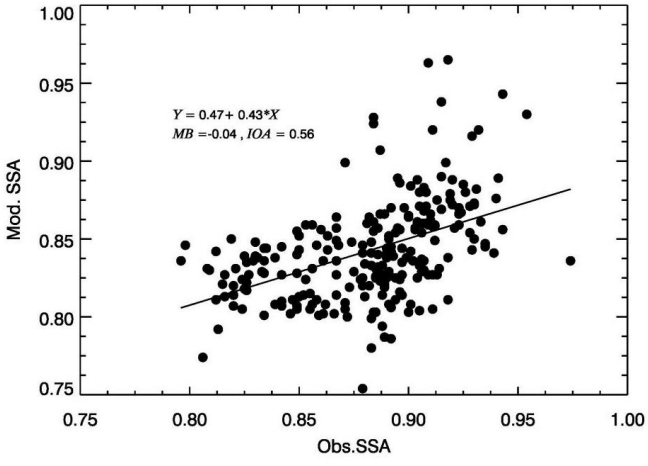

Figure 5. Scatter plot and liner fitting of column integrated SSA at 440 nm

3.2 Surface mass concentrations of BrC in NCP

The simulated distribution of average near-surface BrC concentrations and each source contribution in January 2014 is shown in Fig. 6a. In January, the monthly mean concentrations of BrC in the NCP vary from 0.05 μg m^{-3} to 40.8 μg m^{-3}, with an average of 4.8 μg m^{-3}. The spatial distribution of near-surface BrC concentrations is similar to that of $PM_{2.5}$ in the NCP, with the highest concentration areas located in Hebei Province with an average concentration of 13.5 μg m^{-3}. The simulated BrC concentrations are higher than those reported by Zhu et al. (2021) in 2018, which is perhaps caused by the more severe particulate pollution in January 2014.

https://doi.org/10.5194/egusphere-2024-3468
Preprint. Discussion started: 11 December 2024

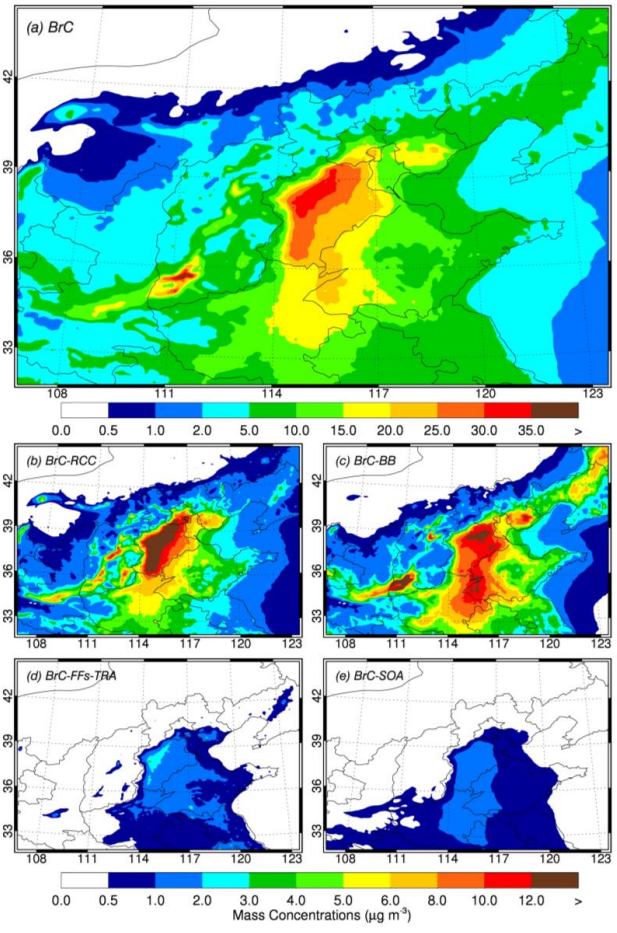

Figure 6. Simulated mean surface concentrations of BrC (a) and each anthropogenic source of RCC (b), of BB (c), of FFs-TRA (d) and secondary BrC (e) in January, 2014 in NCP

Figure 6b-e present the average near-surface BrC concentrations from different anthropogenic sources and secondary formation in January, 2014 in the NCP. The BrC in the NCP predominantly originates from RCC and BB, with an average contribution of 2.3 and 2.9 μg m^{-3} and a maximum of 28.2 and 31.3 μg m^{-3}, respectively. A relatively small proportion of BrC is contributed by FFs-TRA and secondary transformations with an average concentration of 0.5 μg m^{-3} and 0.4 μg m^{-3}, respectively. The BrC from RCC accounts for 46.3% of total BrC concentrations in the NCP, which is highest in Beijing, Hebei, and Tianjin, reaching 63.2%, 48.5% and 47.7% respectively. The BrC from BB counts 41.9% of total BrC concentrations, with the contribution of about 40% in most provinces of the NCP but only 28.9% in Beijing. This result shows that the RCC is one of the major sources

https://doi.org/10.5194/egusphere-2024-3468
Preprint. Discussion started: 11 December 2024

of BrC in NCP due to the wide use of coal for heating and cooking in winter with the low combustion efficiency and fewer emission control. The BrC emitted by RCC is mainly concentrated in the Beijing-Tianjin-Hebei region, while the BrC emitted by BB is distributed in the whole NCP. The Fen-Wei plain exhibits notably high contributions from BB, which is consistent with the emission distribution and with previous studies (Cao and Cui, 2021; Zhang et al., 2021). The Fen-Wei Plain is one of the most densely populated and heavily polluted areas in northern China where biomass is usually used for heating during winter. Although the BrC concentration from FFs-TRA is generally higher in Hebei Province than that in other regions, the highest BrC contribution from FFs-TRA is in Jiangsu Province, reaching up to 16.9%, with an average of 6.1%.

3.3 BrC absorption in the NCP

BrC absorbs visible to near-ultraviolet light with its absorption capabilities extending prominently at shorter wavelengths. Therefore, we calculate the AAOD (aerosol absorption optical depth) to evaluate the absorption contribution of BrC versus bulk aerosols, each anthropogenic source and SOA versus BrC at 365 nm (Fig. 7), by differentiating the AAOD between with and without the contribution of BrC model runs. The average contribution of BrC to the total AAOD of aerosols at 365 nm is11.2% and the maximum is 33.6% in the NCP in January 2014. Compared with the global mean ratio of BrC to BC which is 1.24, the near-surface ratio of that in the NCP is relatively low, with an average of 0.85 because of high concentrations of BC in this area. It is also much lower than that in South America and Africa where BB is generally heavy. On the other hand, although the absorption of BrC in the ultraviolet band is comparable to that of BC, but imaginary index of BrC (about 0.1) is still much lower than that of BC (about 0.76). As a result, the light absorption contribution of BrC at 365 nm is not significant during the study period.

Furthermore, the light absorption properties of BrC during the winter season are predominantly attributed to RCC, followed by BB, SOA, and FFs-TRA in the NCP. The average contribution of RCC and BB to the AAOD of BrC is 55.3% and 26.4%, respectively. Although the concentration of BrC from RCC is comparable to that from BB, the much higher light-absorbing property of the BrC from RCC makes it a dominant contributor to the overall light absorption caused by BrC. The concentration of secondary BrC is lowest compared to that from primary sources, but contributes considerably to BrC AAOD with an average up to 10.6%, which could be explained by its low density and mixing state. The AAOD contribution of BrC from vehicle sources is the lowest, about 3.8% on average, but its contribution in Shanghai and southern Jiangsu ranges from 5% to 10%, higher than in other regions, which is consistent with the its surface mass concentration distribution.

https://doi.org/10.5194/egusphere-2024-3468
Preprint. Discussion started: 11 December 2024

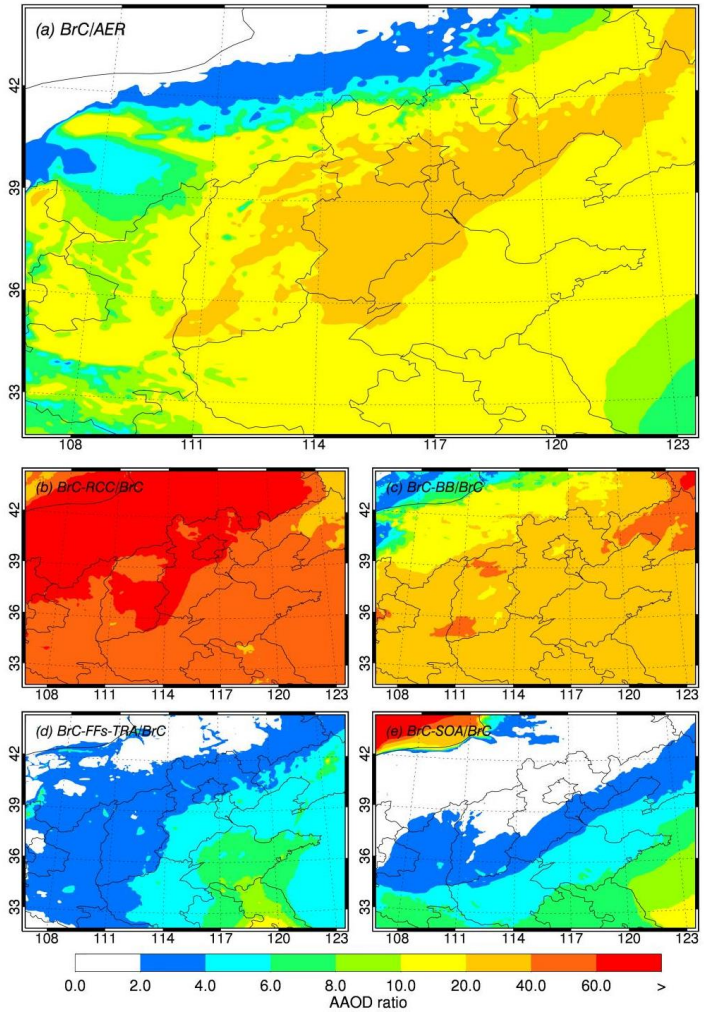

Figure 7 The simulated monthly BrC AAOD versus aerosol at 365nm and each anthropogenic source of RCC, BB, FFs-TRA and secondary BrC AAOD versus BrC in NCP

3.4 Direct radiative effect of BrC

Figure. 8a shows the distribution of the average DRE_{TOA} caused by BrC at the top of the atmosphere during the episode. The DRE_{TOA} in the NCP is -0.10 W m^{-2} on average, with a maximum of +0.45 W m^{-2} and a minimum of -2.45 W m^{-2}. Compared to the average DRE_{TOA} of BC +3.9 W m^{-2} and a maximum of +21.6 W m^{-2}, the average DRE_{TOA} of BrC in the NCP is close to zero. However, in terms of the spatial distribution, the DRE_{TOA} of total BrC in the NCP is predominantly negative, especially in those areas with high BrC concentrations including BTH area

https://doi.org/10.5194/egusphere-2024-3468
Preprint. Discussion started: 11 December 2024

and Fen-wei Plain. The largest negative DRE_{TOA} is in Shanxi province with the highest BrC concentration produced by BB. The results indicate that the overall scattering effect of BrC is greater than its absorption effect, so the BrC populations have a net cooling effect. As we know, the solar irradiance in the UV band contributes only 10% for the total solar irradiation. The imaginary refractive indices of BrC are much lower than those of strongly absorbing BC, especially in the visible band. On the other hand, although these reasons lead to a small heating effect by BrC, the increased DRE_{TOA} induced by BrC which is usually considered as its scattering effect is up to an average of +0.37 W m^{-2} and a maximum of +2.45 W m^{-2} as shown in Fig. 8b. The DRE_{TOA} of OA without BrC is -1.80 W m^{-2} over the NCP (Fig. 8d), and is increased to -1.43 W m^{-2} (Fig. 8c) after considering BrC. Consequently, the cooling effect of OA is reduced by BrC with an average of 24.0%. So far, almost all estimates of the radiation effects of BrC have been based on a global basis. The study of Wang et al. (2014) have shown that the global DRE_{TOA} of BrC is -0.02 W m^{-2}, resulting a DRE_{TOA} increasing of +0.07 W m^{-2}. Brown et al. (2018) have also reported a global annual increased DRE_{TOA} of +0.13 W m^{-2} with the maximum forcing (~+1.75 W m^{-2}) occurs off the west coast of southern Africa. All these estimates only considered BB, biofuels or SOA. This result indicate that the significance of BrC becomes apparent in the estimates for those study typically based on the assumption that OA primarily scatters sun light. The absorption effect of BrC should be considered in climate models to accurately assess the aerosol impact on atmospheric heating and climate change.

https://doi.org/10.5194/egusphere-2024-3468
Preprint. Discussion started: 11 December 2024

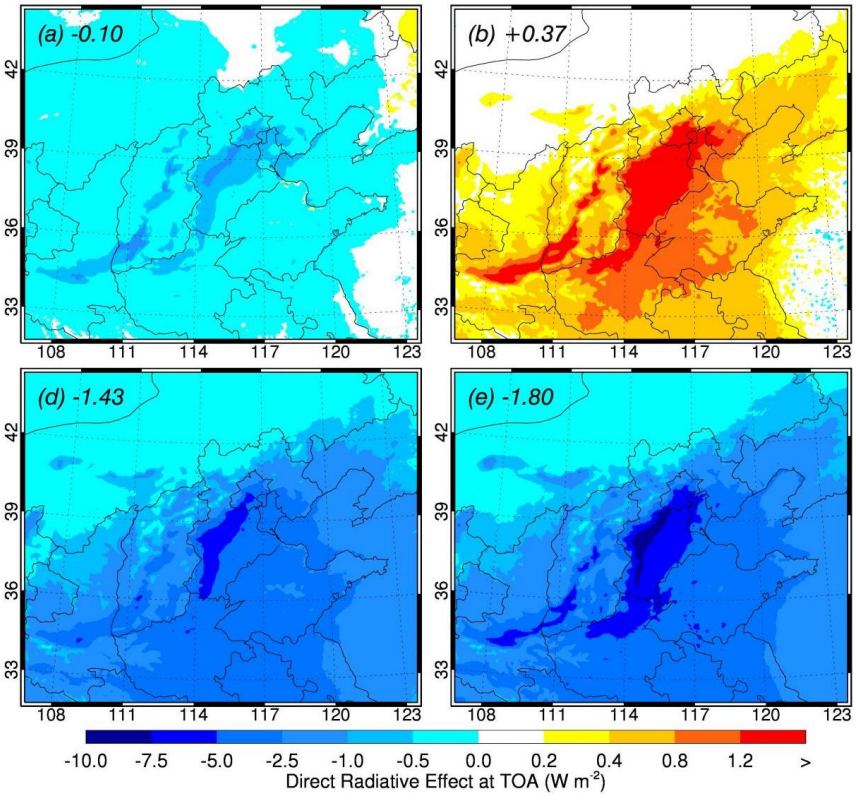

Figure 8, The DRE_{TOA} of BrC (a) and the DRE_{TOA} increase of OA owing to the absorption of BrC (b). The DRE_{TOA} of total OA with absorbing BrC (c) and DRE_{TOA} of total OA with BrC is assumed to be scattering (d). The averages of DRE are shown in the upper left of each panel.

Figure 9a-d shows the estimated DRE_{TOA} of BrC from RCC, BB, FFs-TRA and secondary BrC in the NCP during the episode. Similar to the contribution of BrC sources to the AAOD at 365 nm, the most important source contributing to DRE_{TOA} of BrC is RCC (+0.20 W m^{-2}), followed by BB (+0.11 W m^{-2}), secondary BrC (+0.02 W m^{-2}), and FFs-TRA (+0.01 W m^{-2}) in the NCP, as shown in Fig. 9. However, the DRE_{TOA} of BrC from various sources exhibits distinct spatial distribution characteristics in the NCP. The highest DRE_{TOA} of BrC from fossil sources, which include RCC and FFs-TRA, are predominantly appeared concentrated in Hebei. The highest positive DRE_{TOA} of BrC from BB is found in Fen-Wei Plain. Meanwhile, the secondary BrC contributes most to the DRE_{TOA} in the south part of the NCP. This pattern is likely caused by the high RH levels in the region, which facilitates the internal mixing of secondary BrC with other water-soluble aerosols and aerosol liquid water to enhance its absorption properties.

https://doi.org/10.5194/egusphere-2024-3468
Preprint. Discussion started: 11 December 2024

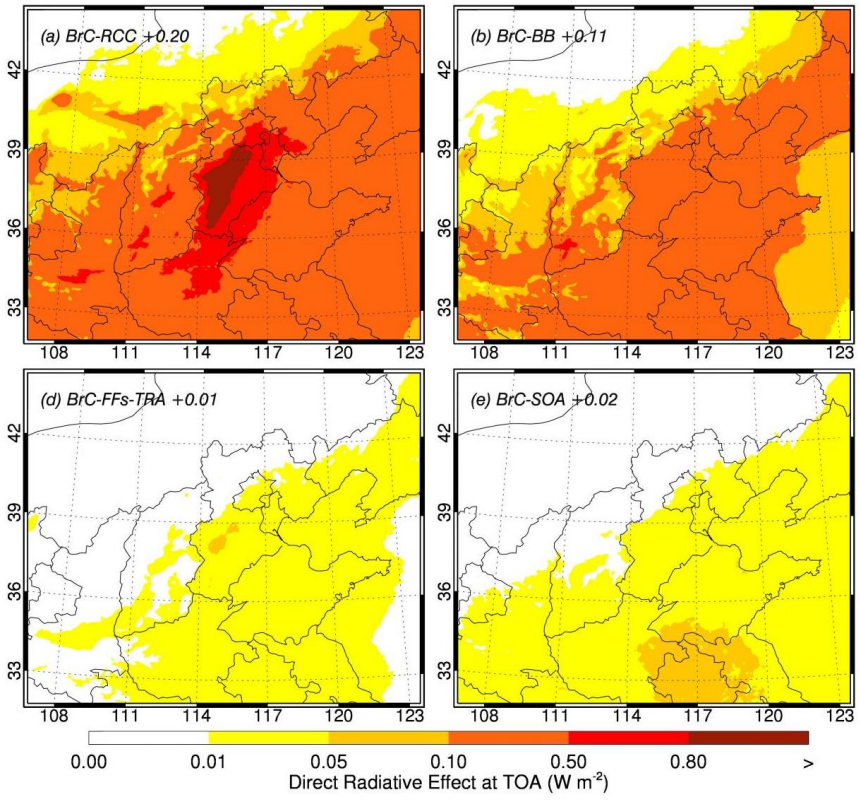

Figure 9. The estimation DRE_{TOA} of each anthropogenic source (a)RCC, (b)BB, (c) FFs-TRA and (d) secondary BrC in NCP in January, 2014

4 Conclusions

A source-explicit BrC simulation in January 2014 in the NCP is conducted by using the WRF-Chem model. We define the BrC based on varying proportions of RCC, BB, FFs-TRA and SOA sources, assigning each a distinct imaginary refractive index to represent their differing light absorption characteristics. Model simulations are evaluated with various data sets. Besides the well reproduction of temporal and spatial variation of aerosol components and SWDOWN in the model, AOD and SSA are used to evaluate the aerosol optical properties.

Near-surface mass concentrations of simulated BrC in the NCP range from 0.05 to 40.8 μg m^{-3} with an average of 4.8 μg m^{-3}, which is mainly contributed by RCC and BB, especially evident in the BTH region and Fen-Wei Plain. Estimation of the BrC contribution to AAOD shows that the BrC accounts for an average of 11.2% and up to 33.6% of the total aerosol absorption at 365 nm. The largest contributor to the absorption of BrC is the

https://doi.org/10.5194/egusphere-2024-3468
Preprint. Discussion started: 11 December 2024

BrC from RCC, reaching 55.3%. BrC generally has a net cooling effect in the NCP if we consider both the absorption and scattering properties, with its DRE_{TOA} of around -0.10 W m^{-2} on average and in the range between -2.45 W m^{-2} and +0.45 W m^{-2}. However, BrC increases the DRE_{TOA} of OA by 24.0% with an average of +0.37 W m^{-2} and up to +2.45 W m^{-2}. The average increased DRE_{TOA} of BrC from RCC, BB, secondary formation, and FFs-TRA is +0.20 W m^{-2}, +0.11 W m^{-2}, +0.02 W m^{-2}, +0.01 W m^{-2}, respectively. The study indicates that although the level of secondary BrC is lower than that of BrC from FFs-TRA, it causes more absorption and larger radiative effects. The pronounced radiative effect of secondary BrC may be not only attributed to their internal mixing with other water-soluble aerosols and aerosol liquid water, but also associated with the relatively low density adopted in the simulation. Although we conducted simulations with low secondary BrC, the impact of secondary BrC on radiative processes should not be overlooked. More field observation and model experiments should be carried out in the future for better understanding of its role in atmospheric radiation balance.

The simulation of BrC in climate models is fraught with uncertainties due to its diverse sources which result in a wide range of optical properties. The absorption characteristics of BrC can change significantly as it undergoes atmospheric aging, impacting its radiative forcing estimates. Additionally, interactions of BrC with other atmospheric particles and its effects on cloud microphysics and albedo introduce further complexities in modeling its climate impact. These uncertainties necessitate enhanced observational data and better integration of BrC properties in climate models to improve the accuracy of climate predictions and assessments. Although the simulations have been evaluated with extensive aerosol mass and optical measurements, more field measurements and lab experiments are needed, especially for the inventory development of BrC, the vertical profiles from aircrafts, and physicochemical properties which would be useful for further evaluating and improving model performance.

Author contributions

Guohui Li and Xuexi Tie designed the study. Jiamao Zhou and Guohui Li wrote the paper. Jiamao Zhou, Jiarui Wu, Xi Li, Ruonan Wang performed the model simulations. Xiaoli Su and Jiang Qian collected the satellite and ground-based observation data. Ting Zhang, Wenting Dai and Junji Cao performed the field observation and laboratory analyze. All authors reviewed and commented on the paper.

https://doi.org/10.5194/egusphere-2024-3468
Preprint. Discussion started: 11 December 2024

Acknowledgments

This work was financially supported by the project of Yong Scientists Fund of the National Natural Science Foundation of China (42107127).

Data availability

The Chinese Ecosystem Research Network (CERN) provided the radiation observation data. The AOD_{550} data is supported from "National Earth System Science Data Center (https://www.geodata.cn)" and AOD_{440} provided by OMI Science Team (https://www.earthdata.nasa.gov/learn/find-data/near-real-time/omi). The SSA data is supported by Sun-sky Radiometer Observation NETwork (http://www.sonet.ac.cn) and the historic profiles of the observed ambient air pollutants provided by Ministry of Ecology and Environment of China (https://www.aqistudy.cn/).

Competing interests

The authors declare that they have no conflict of interest.

https://doi.org/10.5194/egusphere-2024-3468
Preprint. Discussion started: 11 December 2024

References

Andreae, M. O. and Gelencsér, A.: Black carbon or brown carbon?: The nature of light-absorbing carbonaceous aerosols, Atmos. Chem. Phys., 6, 3131–3148, https://doi.org/10.5194/acp-6-3131-2006, 2006.

Bohren, C. F. and Huffman, D. R.: Absorption and Scattering of Light by Small Particles, Wiley, 1998.

Bond, T. C., Doherty, S. J., Fahey, D. W., Forster, P. M., Berntsen, T., DeAngelo, B. J., Flanner, M. G., Ghan, S., Kärcher, B., Koch, D., Kinne, S., Kondo, Y., Quinn, P. K., Sarofim, M. C., Schultz, M. G., Schulz, M., Venkataraman, C., Zhang, H., Zhang, S., Bellouin, N., Guttikunda, S. K., Hopke, P. K., Jacobson, M. Z., Kaiser, J. W., Klimont, Z., Lohmann, U., Schwarz, J. P., Shindell, D., Storelvmo, T., Warren, S. G., and Zender, C. S.: Bounding the role of black carbon in the climate system: A scientific assessment, J. Geophys. Res., 118, 5380–5552, https://doi.org/10.1002/jgrd.50171, 2013.

Bond, T. C.: Spectral dependence of visible light absorption by carbonaceous particles emitted from coal combustion, Geophys. Res. Lett., 28, 4075–4078, https://doi.org/10.1029/2001GL013652, 2001.

Brown, H., Liu, X., Feng, Y., Jiang, Y., Wu, M., Lu, Z., Wu, C., Murphy, S., and Pokhrel, R.: Radiative effect and climate impacts of brown carbon with the Community Atmosphere Model (CAM5), Atmos. Chem. Phys., 18, 17745–17768, https://doi.org/10.5194/acp-18-17745-2018, 2018.

Browne, E. C., Zhang, X., Franklin, J. P., Ridley, K. J., Kirchstetter, T. W., Wilson, K. R., Cappa, C. D., and Kroll, J. H.: Effect of heterogeneous oxidative aging on light absorption by biomass burning organic aerosol, Aerosol Science and Technology, 53, 663–674, https://doi.org/10.1080/02786826.2019.1599321, 2019.

Cao, J. J. and Cui, L.: Current Status, Characteristics and Causes of Particulate Air Pollution in the Fenwei Plain, China: A Review, J. Geophys. Res., 126, https://doi.org/10.1029/2020JD034472, 2021.

Chand, D., Wood, R., Ghan, S. J., Wang, M., Ovchinnikov, M., Rasch, P. J., Miller, S., Schichtel, B., and Moore, T.: Aerosol optical depth increase in partly cloudy conditions, J. Geophys. Res., 117, https://doi.org/10.1029/2012JD017894, 2012.

Chen, W., Wang, Z., Zhao, H., and Qin, K.: A novel way to calculate shortwave black carbon direct radiative effect, The Science of the total environment, 756, 142961, https://doi.org/10.1016/j.scitotenv.2020.142961, 2021.

Du, Z., He, K., Cheng, Y., Duan, F., Ma, Y., Liu, J., Zhang, X., Zheng, M., and Weber, R.: A yearlong study of water-soluble organic carbon in Beijing II: Light absorption properties, Atmospheric Environment, 89, 235–241, https://doi.org/10.1016/j.atmosenv.2014.02.022, 2014.

https://doi.org/10.5194/egusphere-2024-3468
Preprint. Discussion started: 11 December 2024

396 Fast, J. D., Gustafson, W. I., Easter, R. C., Zaveri, R. A., Barnard, J. C., Chapman, E. G., Grell, G. A., and
397 Peckham, S. E.: Evolution of ozone, particulates, and aerosol direct radiative forcing in the vicinity of Houston
398 using a fully coupled meteorology-chemistry-aerosol model, J. Geophys. Res., 111, 2981,
399 https://doi.org/10.1029/2005JD006721, 2006.
400 Feng, Y., Ramanathan, V., and Kotamarthi, V. R.: Brown carbon: A significant atmospheric absorber of solar
401 radiation?, 2013.
402 Grell, G. A., Peckham, S. E., Schmitz, R., McKeen, S. A., Frost, G., Skamarock, W. C., and Eder, B.: Fully
403 coupled "online" chemistry within the WRF model, Atmospheric Environment, 39, 6957–6975,
404 https://doi.org/10.1016/j.atmosenv.2005.04.027, 2005.
405 Guenther, A., Karl, T., Harley, P., Wiedinmyer, C., Palmer, P. I., and Geron, C.: Estimates of global terrestrial
406 isoprene emissions using MEGAN (Model of Emissions of Gases and Aerosols from Nature), Atmos. Chem.
407 Phys., 6, 3181–3210, https://doi.org/10.5194/acp-6-3181-2006, 2006.
408 Hammer, M. S., Martin, R. V., van Donkelaar, A., Buchard, V., Torres, O., Ridley, D. A., and Spurr, R. J. D.:
409 Interpreting the ultraviolet aerosol index observed with the OMI satellite instrument to understand absorption by
410 organic aerosols: Implications for atmospheric oxidation and direct radiative effects, Atmos. Chem. Phys., 16,
411 2507–2523, https://doi.org/10.5194/acp-16-2507-2016, 2016.
412 Hecobian, A., Zhang, X., Zheng, M., Frank, N., Edgerton, E. S., and Weber, R. J.: Water-Soluble Organic
413 Aerosol material and the light-absorption characteristics of aqueous extracts measured over the Southeastern
414 United States, Atmos. Chem. Phys., 10, 5965–5977, https://doi.org/10.5194/acp-10-5965-2010, 2010.
415 Hoffer, A., Gelencsér, A., Guyon, P., Kiss, G., Schmid, O., Frank, G. P., Artaxo, P., and Andreae, M. O.: Optical
416 properties of humic-like substances (HULIS) in biomass-burning aerosols, Atmos. Chem. Phys., 6, 3563–3570,
417 https://doi.org/10.5194/acp-6-3563-2006, 2006.
418 Hu, Z., Kang, S., Li, C., Yan, F., Chen, P., Gao, S., Wang, Z., Zhang, Y., and Sillanpää, M.: Light absorption of
419 biomass burning and vehicle emission-sourced carbonaceous aerosols of the Tibetan Plateau, Environmental
420 science and pollution research international, 24, 15369–15378, https://doi.org/10.1007/s11356-017-9077-3,
421 2017.
422 Huang, R.-j., Yuan, W., Yang, L., Yang, H., Cao, W., Guo, J., Zhang, N., Zhu, C., Wu, Y., and Zhang, R.:
423 Concentration, optical characteristics, and emission factors of brown carbon emitted by on-road vehicles, The
424 Science of the total environment, 810, 151307, https://doi.org/10.1016/j.scitotenv.2021.151307, 2022.

https://doi.org/10.5194/egusphere-2024-3468
Preprint. Discussion started: 11 December 2024

Huang, X., Song, Y., Zhao, C., Cai, X., Zhang, H., and Zhu, T.: Direct Radiative Effect by Multicomponent Aerosol over China*, Journal of Climate, 28, 3472–3495, https://doi.org/10.1175/JCLI-D-14-00365.1, 2015.

IPCC (Ed.): Climate Change 2013: The Physical Science Basis. Contribution of Working Group I to the Fifth Assessment Report of the Intergovernmental Panel on Climate Change, Cambridge University Press, Cambridge, United Kingdom and New York, NY, USA, 2013.

Jacobson, M. Z.: Effects of biomass burning on climate, accounting for heat and moisture fluxes, black and brown carbon, and cloud absorption effects, J. Geophys. Res., 119, 8980–9002, https://doi.org/10.1002/2014JD021861, 2014.

Jeong, J. I., Jo, D. S., Park, R. J., Lee, H.-M., Curci, G., and Kim, S.-W.: Parametric analysis for global single scattering albedo calculations, Atmospheric Environment, 234, 117616, https://doi.org/10.1016/j.atmosenv.2020.117616, 2020.

Jo, D. S., Park, R. J., Lee, S., Kim, S.-W., and Zhang, X.: A global simulation of brown carbon: Implications for photochemistry and direct radiative effect, Atmos. Chem. Phys., 16, 3413–3432, https://doi.org/10.5194/acp-16-3413-2016, 2016.

Kirchstetter, T. W., Novakov, T., and Hobbs, P. V.: Evidence that the spectral dependence of light absorption by aerosols is affected by organic carbon, J. Geophys. Res., 109, n/a-n/a, https://doi.org/10.1029/2004JD004999, 2004.

Li, C., He, Q., Hettiyadura, A. P. S., Käfer, U., Shmul, G., Meidan, D., Zimmermann, R., Brown, S. S., George, C., Laskin, A., and Rudich, Y.: Formation of Secondary Brown Carbon in Biomass Burning Aerosol Proxies through NO3 Radical Reactions, Environmental science & technology, 54, 1395–1405, https://doi.org/10.1021/acs.est.9b05641, 2020.

Li, G., Lei, W., Bei, N., and Molina, L. T.: Contribution of garbage burning to chloride and $PM_{2.5}$ in Mexico City, Atmos. Chem. Phys., 12, 8751–8761, https://doi.org/10.5194/acp-12-8751-2012, 2012.

Li, G., Bei, N., Tie, X., and Molina, L. T.: Aerosol effects on the photochemistry in Mexico City during MCMA-2006/MILAGRO campaign, Atmos. Chem. Phys., 11, 5169–5182, https://doi.org/10.5194/acp-11-5169-2011, 2011a.

Li, G., Zavala, M., Lei, W., Tsimpidi, A. P., Karydis, V. A., Pandis, S. N., Canagaratna, M. R., and Molina, L. T.: Simulations of organic aerosol concentrations in Mexico City using the WRF-CHEM model during the MCMA-2006/MILAGRO campaign, Atmos. Chem. Phys., 11, 3789–3809, https://doi.org/10.5194/acp-11-3789-2011,

https://doi.org/10.5194/egusphere-2024-3468
Preprint. Discussion started: 11 December 2024

2011b.

Li, G., Lei, W., Zavala, M., Volkamer, R., Dusanter, S., Stevens, P., and Molina, L. T.: Impacts of HONO sources on the photochemistry in Mexico City during the MCMA-2006/MILAGO Campaign, Atmos. Chem. Phys., 10, 6551–6567, https://doi.org/10.5194/acp-10-6551-2010, 2010.

Li, G., Bei, N., Cao, J., Wu, J., Long, X., Feng, T., Dai, W., Liu, S., Zhang, Q., and Tie, X.: Widespread and persistent ozone pollution in eastern China during the non-winter season of 2015: observations and source attributions, Atmos. Chem. Phys., 17, 2759–2774, https://doi.org/10.5194/acp-17-2759-2017, 2017.

Li, M., Fan, X., Zhu, M., Zou, C., Song, J., Wei, S., Jia, W., and Peng, P.'a.: Abundance and Light Absorption Properties of Brown Carbon Emitted from Residential Coal Combustion in China, Environmental science & technology, 53, 595–603, https://doi.org/10.1021/acs.est.8b05630, 2019.

Lin, G., Penner, J. E., Flanner, M. G., Sillman, S., Xu, L., and Zhou, C.: Radiative forcing of organic aerosol in the atmosphere and on snow: Effects of SOA and brown carbon, J. Geophys. Res., 119, 7453–7476, https://doi.org/10.1002/2013JD021186, 2014.

Liu, D., Whitehead, J., Alfarra, M. R., Reyes-Villegas, E., Spracklen, D. V., Reddington, C. L., Kong, S., Williams, P. I., Ting, Y.-C., Haslett, S., Taylor, J. W., Flynn, M. J., Morgan, W. T., McFiggans, G., Coe, H., and Allan, J. D.: Black-carbon absorption enhancement in the atmosphere determined by particle mixing state, Nature Geosci, 10, 184–188, https://doi.org/10.1038/ngeo2901, 2017.

Liu, J., Bergin, M., Guo, H., King, L., Kotra, N., Edgerton, E., and Weber, R. J.: Size-resolved measurements of brown carbon in water and methanol extracts and estimates of their contribution to ambient fine-particle light absorption, Atmos. Chem. Phys., 13, 12389–12404, https://doi.org/10.5194/acp-13-12389-2013, 2013.

Liu, J., Lin, P., Laskin, A., Laskin, J., Kathmann, S. M., Wise, M., Caylor, R., Imholt, F., Selimovic, V., and Shilling, J. E.: Optical properties and aging of light-absorbing secondary organic aerosol, Atmos. Chem. Phys., 16, 12815–12827, https://doi.org/10.5194/acp-16-12815-2016, 2016.

Liu, P. F., Abdelmalki, N., Hung, H.-M., Wang, Y., Brune, W. H., and Martin, S. T.: Ultraviolet and visible complex refractive indices of secondary organic material produced by photooxidation of the aromatic compounds toluene and m-xylene, Atmos. Chem. Phys., 15, 1435–1446, https://doi.org/10.5194/acp-15-1435-2015, 2015.

Lu, Z., Streets, D. G., Winijkul, E., Yan, F., Chen, Y., Bond, T. C., Feng, Y., Dubey, M. K., Liu, S., Pinto, J. P., and Carmichael, G. R.: Light absorption properties and radiative effects of primary organic aerosol emissions,

https://doi.org/10.5194/egusphere-2024-3468
Preprint. Discussion started: 11 December 2024

Environmental science & technology, 49, 4868–4877, https://doi.org/10.1021/acs.est.5b00211, 2015.

Mo, Y., Li, J., Cheng, Z., Zhong, G., Zhu, S., Tian, C., Chen, Y., and Zhang, G.: Dual Carbon Isotope-Based Source Apportionment and Light Absorption Properties of Water-Soluble Organic Carbon in PM 2.5 Over China, JGR Atmospheres, 126, 27805, https://doi.org/10.1029/2020JD033920, 2021.

Mukai, H. and Ambe, Y.: Characterization of a humic acid-like brown substance in airborne particulate matter and tentative identification of its origin, Atmospheric Environment (1967), 20, 813–819, https://doi.org/10.1016/0004-6981(86)90265-9, 1986.

Ni, H., Huang, R.-j., Pieber, S. M., Corbin, J. C., Stefenelli, G., Pospisilova, V., Klein, F., Gysel-Beer, M., Yang, L., Baltensperger, U., Haddad, I. E., Slowik, J. G., Cao, J., Prévôt, A. S. H., and Dusek, U.: Brown Carbon in Primary and Aged Coal Combustion Emission, Environmental science & technology, 55, 5701–5710, https://doi.org/10.1021/acs.est.0c08084, 2021.

Park, R. J., Kim, M. J., Jeong, J. I., Youn, D., and Kim, S.: A contribution of brown carbon aerosol to the aerosol light absorption and its radiative forcing in East Asia, Atmospheric Environment, 44, 1414–1421, https://doi.org/10.1016/j.atmosenv.2010.01.042, 2010.

Pokhrel, R. P., Beamesderfer, E. R., Wagner, N. L., Langridge, J. M., Lack, D. A., Jayarathne, T., Stone, E. A., Stockwell, C. E., Yokelson, R. J., and Murphy, S. M.: Relative importance of black carbon, brown carbon, and absorption enhancement from clear coatings in biomass burning emissions, Atmos. Chem. Phys., 17, 5063–5078, https://doi.org/10.5194/acp-17-5063-2017, 2017.

Saleh, R.: From Measurements to Models: Toward Accurate Representation of Brown Carbon in Climate Calculations, Curr Pollution Rep, 6, 90–104, https://doi.org/10.1007/s40726-020-00139-3, 2020.

Saleh, R., Robinson, E. S., Tkacik, D. S., Ahern, A. T., Liu, S., Aiken, A. C., Sullivan, R. C., Presto, A. A., Dubey, M. K., Yokelson, R. J., Donahue, N. M., and Robinson, A. L.: Brownness of organics in aerosols from biomass burning linked to their black carbon content, Nature Geosci, 7, 647–650, https://doi.org/10.1038/ngeo2220, 2014.

Satheesh, S. K., Vinoj, V., and Krishnamoorthy, K.: Assessment of Aerosol Radiative Impact over Oceanic Regions Adjacent to Indian Subcontinent Using Multisatellite Analysis, Advances in Meteorology, 2010, 1–13, https://doi.org/10.1155/2010/139186, 2010.

Shapiro, E. L., Szprengiel, J., Sareen, N., Jen, C. N., Giordano, M. R., and McNeill, V. F.: Light-absorbing secondary organic material formed by glyoxal in aqueous aerosol mimics, Atmos. Chem. Phys., 9, 2289–2300,

https://doi.org/10.5194/egusphere-2024-3468
Preprint. Discussion started: 11 December 2024

https://doi.org/10.5194/acp-9-2289-2009, 2009.

Song, S., Wang, Y., Wang, Y., Wang, T., and Tan, H.: The characteristics of particulate matter and optical properties of Brown carbon in air lean condition related to residential coal combustion, Powder Technology, 379, 505–514, https://doi.org/10.1016/j.powtec.2020.10.082, 2021.

Sun, J., Zhang, Y., Zhi, G., Hitzenberger, R., Jin, W., Chen, Y., Wang, L., Tian, C., Li, Z., Chen, R., Xiao, W., Cheng, Y., Yang, W., Yao, L., Cao, Y., Huang, D., Qiu, Y., Xu, J., Xia, X., Yang, X., Zhang, X., Zong, Z., Song, Y., and Wu, C.: Brown carbon's emission factors and optical characteristics in household biomass burning: Developing a novel algorithm for estimating the contribution of brown carbon, Atmos. Chem. Phys., 21, 2329–2341, https://doi.org/10.5194/acp-21-2329-2021, 2021.

Sun, J., Zhi, G., Hitzenberger, R., Chen, Y., Tian, C., Zhang, Y., Feng, Y., Cheng, M., Zhang, Y., Cai, J., Chen, F., Qiu, Y., Jiang, Z., Li, J., Zhang, G., and Mo, Y.: Emission factors and light absorption properties of brown carbon from household coal combustion in China, Atmos. Chem. Phys., 17, 4769–4780, https://doi.org/10.5194/acp-17-4769-2017, 2017.

Tang, J., Li, J., Su, T., Han, Y., Mo, Y., Jiang, H., Cui, M., Jiang, B., Chen, Y., Tang, J., Song, J., Peng, P.'a., and Zhang, G.: Molecular compositions and optical properties of dissolved brown carbon in biomass burning, coal combustion, and vehicle emission aerosols illuminated by excitation–emission matrix spectroscopy and Fourier transform ion cyclotron resonance mass spectrometry analysis, Atmos. Chem. Phys., 20, 2513–2532, https://doi.org/10.5194/acp-20-2513-2020, 2020.

Tian, J., Wang, Q., Ni, H., Wang, M., Zhou, Y., Han, Y., Shen, Z., Pongpiachan, S., Zhang, N., Zhao, Z., Zhang, Q., Zhang, Y., Long, X., and Cao, J.: Emission Characteristics of Primary Brown Carbon Absorption From Biomass and Coal Burning: Development of an Optical Emission Inventory for China, J. Geophys. Res. Atmos., 15, 27,805, https://doi.org/10.1029/2018JD029352, 2019.

Tuccella, P., Curci, G., Pitari, G., Lee, S., and Jo, D. S.: Direct Radiative Effect of Absorbing Aerosols: Sensitivity to Mixing State, Brown Carbon, and Soil Dust Refractive Index and Shape, J. Geophys. Res. Atmos., 125, 317, https://doi.org/10.1029/2019JD030967, 2020.

Wang, J., Ye, J., Zhang, Q., Zhao, J., Wu, Y., Li, J., Liu, D., Li, W., Zhang, Y., Wu, C., Xie, C., Qin, Y., Lei, Y., Huang, X., Guo, J., Liu, P., Fu, P., Li, Y., Lee, H. C., Choi, H., Zhang, J., Liao, H., Chen, M., Sun, Y., Ge, X., Martin, S. T., and Jacob, D. J.: Aqueous production of secondary organic aerosol from fossil-fuel emissions in winter Beijing haze, Proceedings of the National Academy of Sciences of the United States of America, 118,

https://doi.org/10.5194/egusphere-2024-3468
Preprint. Discussion started: 11 December 2024

https://doi.org/10.1073/pnas.2022179118, 2021.

Wang, Q., Zhou, Y., Ma, N., Zhu, Y., Zhao, X., Zhu, S., Tao, J., Hong, J., Wu, W., Cheng, Y., and Su, H.: Review of Brown Carbon Aerosols in China: Pollution Level, Optical Properties, and Emissions, JGR Atmospheres, 127, 455, https://doi.org/10.1029/2021JD035473, 2022.

Wang, Q., Ye, J., Wang, Y., Zhang, T., Ran, W., Wu, Y., Tian, J., Li, L., Zhou, Y., Hang Ho, S. S., Dang, B., Zhang, Q., Zhang, R., Chen, Y., Zhu, C., and Cao, J.: Wintertime Optical Properties of Primary and Secondary Brown Carbon at a Regional Site in the North China Plain, Environmental science & technology, 53, 12389–12397, https://doi.org/10.1021/acs.est.9b03406, 2019.

Wang, X., Heald, C. L., Ridley, D. A., Schwarz, J. P., Spackman, J. R., Perring, A. E., Coe, H., Liu, D., and Clarke, A. D.: Exploiting simultaneous observational constraints on mass and absorption to estimate the global direct radiative forcing of black carbon and brown carbon, Atmos. Chem. Phys., 14, 10989–11010, https://doi.org/10.5194/acp-14-10989-2014, 2014.

Wang, X., Heald, C. L., Liu, J., Weber, R. J., Campuzano-Jost, P., Jimenez, J. L., Schwarz, J. P., and Perring, A. E.: Exploring the observational constraints on the simulation of brown carbon, Atmos. Chem. Phys., 18, 635–653, https://doi.org/10.5194/acp-18-635-2018, 2018.

Wang, Y., Wang, Y., Song, S., Wang, T., Li, D., and Tan, H.: Effects of coal types and combustion conditions on carbonaceous aerosols in flue gas and their light absorption properties, Fuel, 277, 118148, https://doi.org/10.1016/j.fuel.2020.118148, 2020.

Wu, J., Bei, N., Hu, B., Liu, S., Wang, Y., Shen, Z., Li, X., Liu, L., Wang, R., Liu, Z., Cao, J., Tie, X., Molina, L. T., and Li, G.: Aerosol-photolysis interaction reduces particulate matter during wintertime haze events, Proceedings of the National Academy of Sciences of the United States of America, 117, 9755–9761, https://doi.org/10.1073/pnas.1916775117, 2020.

Xie, C., Xu, W., Wang, J., Wang, Q., Liu, D., Tang, G., Chen, P., Du, W., Zhao, J., Zhang, Y., Zhou, W., Han, T., Bian, Q., Li, J., Fu, P., Wang, Z., Ge, X., Allan, J., Coe, H., and Sun, Y.: Vertical characterization of aerosol optical properties and brown carbon in winter in urban Beijing, China, Atmos. Chem. Phys., 19, 165–179, https://doi.org/10.5194/acp-19-165-2019, 2019.

Xie, M., Hays, M. D., and Holder, A. L.: Light-absorbing organic carbon from prescribed and laboratory biomass burning and gasoline vehicle emissions, Scientific reports, 7, 7318, https://doi.org/10.1038/s41598-017-06981-8, 2017a.

https://doi.org/10.5194/egusphere-2024-3468
Preprint. Discussion started: 11 December 2024

570 Xie, M., Chen, X., Hays, M. D., Lewandowski, M., Offenberg, J., Kleindienst, T. E., and Holder, A. L.: Light
571 Absorption of Secondary Organic Aerosol: Composition and Contribution of Nitroaromatic Compounds,
572 Environmental science & technology, 51, 11607–11616, https://doi.org/10.1021/acs.est.7b03263, 2017b.
573 Yan, C., Zheng, M., Bosch, C., Andersson, A., Desyaterik, Y., Sullivan, A. P., Collett, J. L., Zhao, B., Wang, S.,
574 He, K., and Gustafsson, Ö.: Important fossil source contribution to brown carbon in Beijing during winter,
575 Scientific reports, 7, 43182, https://doi.org/10.1038/srep43182, 2017.
576 Yan, J., Wang, X., Gong, P., Wang, C., and Cong, Z.: Review of brown carbon aerosols: Recent progress and
577 perspectives, The Science of the total environment, 634, 1475–1485,
578 https://doi.org/10.1016/j.scitotenv.2018.04.083, 2018.
579 Yan, Q., Kong, S., Yan, Y., Liu, X., Zheng, S., Qin, S., Wu, F., Niu, Z., Zheng, H., Cheng, Y., Zeng, X., Wu, J.,
580 Yao, L., Liu, D., and Qi, S.: Hourly emission estimation of black carbon and brown carbon absorption from
581 domestic coal burning in China, The Science of the total environment, 814, 151950,
582 https://doi.org/10.1016/j.scitotenv.2021.151950, 2022.
583 Yang, M., Howell, S. G., Zhuang, J., and Huebert, B. J.: Attribution of aerosol light absorption to black carbon,
584 brown carbon, and dust in China – interpretations of atmospheric measurements during EAST-AIRE, Atmos.
585 Chem. Phys., 9, 2035–2050, https://doi.org/10.5194/acp-9-2035-2009, 2009.
586 Zhang, A., Wang, Y., Zhang, Y., Weber, R. J., Song, Y., Ke, Z., and Zou, Y.: Modeling the global radiative effect
587 of brown carbon: A potentially larger heating source in the tropical free troposphere than black carbon, Atmos.
588 Chem. Phys., 20, 1901–1920, https://doi.org/10.5194/acp-20-1901-2020, 2020.
589 Zhang, Q., Streets, D. G., Carmichael, G. R., He, K. B., Huo, H., Kannari, A., Klimont, Z., Park, I. S., Reddy, S.,
590 Fu, J. S., Chen, D., Duan, L., Lei, Y., Wang, L. T., and Yao, Z. L.: Asian emissions in 2006 for the NASA
591 INTEX-B mission, Atmos. Chem. Phys., 9, 5131–5153, https://doi.org/10.5194/acp-9-5131-2009, 2009.
592 Zhang, W., Wang, W., Li, J., Ma, S., Lian, C., Li, K., Shi, B., Liu, M., Li, Y., Wang, Q., Sun, Y., Tong, S., and
593 Ge, M.: Light absorption properties and potential sources of brown carbon in Fenwei Plain during winter 2018-
594 2019, Journal of environmental sciences (China), 102, 53–63, https://doi.org/10.1016/j.jes.2020.09.007, 2021.
595 Zhang, Y., Wang, Q., Tian, J., Li, Y., Liu, H., Ran, W., Han, Y., Prévôt, A. S.H., and Cao, J.: Impact of COVID-
596 19 lockdown on the optical properties and radiative effects of urban brown carbon aerosol, Geoscience
597 Frontiers, 13, 101320, https://doi.org/10.1016/j.gsf.2021.101320, 2022.
598 Zhao, C., Ruby Leung, L., Easter, R., Hand, J., and Avise, J.: Characterization of speciated aerosol direct

https://doi.org/10.5194/egusphere-2024-3468
Preprint. Discussion started: 11 December 2024

599 radiative forcing over California, JGR Atmospheres, 118, 2372–2388, https://doi.org/10.1029/2012JD018364,
600 2013.
601 Zhu, Y., Wang, Q., Yang, X., Yang, N., and Wang, X.: Modeling Investigation of Brown Carbon Aerosol and Its
602 Light Absorption in China, Atmosphere, 12, 892, https://doi.org/10.3390/atmos12070892, 2021.
603